

Controllers coordination for diesel engines NOx emissions management

*Original*

Controllers coordination for diesel engines NOx emissions management / Ventura, Loris; Malan, Stefano.. - ELETTRONICO. - 2023 31st Mediterranean Conference on Control and Automation (MED):(2023), pp. 440-445. (Intervento presentato al convegno 2023 31st Mediterranean Conference on Control and Automation (MED) tenutosi a Limassol, Cyprus nel June 26-29, 2023) [10.1109/MED59994.2023.10185886].

*Availability:*

This version is available at: 11583/2980729 since: 2023-10-21T13:48:44Z

*Publisher:*

IEEE

*Published*

DOI:10.1109/MED59994.2023.10185886

*Terms of use:*

This article is made available under terms and conditions as specified in the corresponding bibliographic description in the repository

*Publisher copyright*

IEEE postprint/Author's Accepted Manuscript

©2023 IEEE. Personal use of this material is permitted. Permission from IEEE must be obtained for all other uses, in any current or future media, including reprinting/republishing this material for advertising or promotional purposes, creating new collecting works, for resale or lists, or reuse of any copyrighted component of this work in other works.

(Article begins on next page)

# Controllers coordination for diesel engines NOx emissions management

Loris Ventura<sup>1</sup> and Stefano A. Malan<sup>2</sup>

**Abstract**—Tightened diesel pollutants emissions regulations rendered the performance of steady-state map controls, which are commonly used in Internal Combustion Engine (ICE) management, unsatisfactory. To overcome these performance constraints, control systems must deal with engine transient operation, subsystem coupling and the trade-off between different requirements to efficiently manage the engine. The research demonstrates the utility of a reference generator for coordinating the air path and combustion control systems of a turbocharged diesel engine for heavy-duty applications. The control system coordinator is based on neural networks and allows following different engine-out Nitrogen Oxides (NOx) targets while satisfying the load request. The main idea is to generate air path targets, intake  $O_2$  concentration and Intake Manifold Pressure (IMAP), in accordance with the ones of the combustion control system, engine load, in the form of Brake Mean Effective Pressure (BMEP), and NOx. As a result, the air path control system provides the global conditions for the engine proper operation, while the combustion control responds to rapid changes in the engine operating state and compensates for any remaining deviations from load and NOx targets. The reference generator, as well as the two controllers, are suitable for real-time implementation on rapid-prototyping hardware. The performance was overall good, achieving average deviations of 0.1 bar for the BMEP and 150 ppm for the NOx.

## I. INTRODUCTION

The ICE pollutants emission regulations tighten as the transition to green and sustainable transportation systems spreads. Recognizing this, automotive manufacturers have introduced a wide range of technologies, particularly for diesel engines: Exhaust Gas Recirculation (EGR) with Variable Geometry Turbochargers (VGTs) [1], high-pressure common rail injection systems [2], advanced combustion control and alternative combustion concepts [3], [4], for example. Recently, the focus of diesel engine research has shifted toward the development of modern control strategies such as [4], [5]. This was supported by increased computational performance of Engine Control Units (ECUs).

The importance of an air path and combustion controllers coordinator cannot be ignored. Targets for the two control systems must be developed while taking into account their different time dynamics and actual working conditions. The main reason for the sometime poor performance of the two control systems is the mismatch between the actual and reference values of key variables used for the target generation. The two control systems are independent, but the air path and combustion subsystems are strongly coupled and, with

this bias, the two controlled systems will work in conditions that differ from the expected ones.

In this work, a coordinator constituted by neural networks has been used to manage the air path and combustion control systems through their respective target signals. The coordinator generates a target for the air path control system based on a desired set point, the state of the engine and injection control system. The design choice was to use the air path control system to provide the global conditions needed to fulfill the performance request and the injection control system to locally adjust the remaining part and react fast to perturbations while guaranteeing the load.

By looking at the literature, only few examples of air path and combustion control systems coordinators arose. In [6] controllers were coordinated by a high level structure that considered as states combustion halfway point, peak pressure, combustion rate and instability and Indicated Mean Effective Pressure (IMEP) obtained from in-cylinder pressure measurement to generate the correct references. A dedicated PI control loop was applied to each cylinder to manage fuel quantity and Start Of Injection (SOI). Instead, the air path controller targeted Air Mass Flow rate (MAF) and IMAP.

In [7] a supervisory model predictive control (MPC) is developed for an air path system in a diesel engine; in it three parts work together to manage the nonlinear controllers: target coordinator, actuator nonlinear control and state detection. By modeling the coordination dynamics as a set of first order transfer functions, the system is more efficient and reliable.

Paper [8] regulates both air path and combustion in a diesel engine running partially premixed combustion. In the air path, MAF and IMAP are regulated through EGR and VGT actuators. While the combustion is managed through the main injection duration. The control structure featured an MPC with a Kalman filter that compensates the model errors. Still, the references for the target variables were coming from maps and models obtained from a sensitivity analysis.

The control systems used on ICEs are typically feed-forward, relying on steady-state maps, or closed-loop via the use of PIDs [9]. These control systems are ineffective, especially during transient operations. Nonetheless, their advantages of simple design and implementation led to their widespread adoption by the industry. However, the reduction in pollutant emissions mandated by current regulations has pushed the development of modern model-based controllers. Several model-based controller examples have been published in the literature, including Multiple Input Multiple Output (MIMO) eigenvalue placement [10] and predictive control [12]; also strategies as neural network and fuzzy control [12] are of interest regardless their complexity and counter-intuitive

\*This work was not supported by any organization

<sup>1</sup> Loris Ventura is with Energy Department, Politecnico di Torino, Torino, Italy. [loris.ventura@polito.it](mailto:loris.ventura@polito.it)

<sup>2</sup> Stefano A. Malan is with the Dept. of Electronics and Telecommunications, Politecnico di Torino, Torino, Italy. [stefano.malan@polito.it](mailto:stefano.malan@polito.it)

TABLE I  
ENGINE MAIN SPECIFICATIONS

Engine type	Euro VI diesel
Number of cylinders	4
Displacement	2998 cm <sup>3</sup>
Bore x stroke	95.8 x 104 mm
Rod length	160 mm
Compression ratio	17.5 : 1
Valves per cylinder	4
Turbocharger	VGT type
Fuel injection system	High Pressure Common Rail

parameter tuning.

The targeted variables, in addition to the control layout, are critical. Instead of the fresh MAF, the intake  $O_2$  concentration was chosen as a controlled variable in this study. This is due to the MAF not being strictly correlated to NOx pollutants. As a result, emission control through its use is difficult and ineffective [10].

Still, the benefits deriving from the employment of these control methodologies could be compromised by the lack of coherent references that are provided to them.

In this paper, section 2, the engine together with the air path, combustion control systems and their coordinator are briefly described and referenced for more details. Section 3 presents the results of Model-in-the-Loop (MiL) tests with the employment of the coordinated structure over transient tests. Section 4 provides the conclusion of the work.

## II. OVERALL CONTROL STRUCTURE

The engine considered in this work is a 3-liter EURO VI diesel: Table I lists its key specifications. The engine layout features a High-Pressure EGR (HP-EGR), EGR cooler, VGT, Exhaust flap and Intercooler, Fig. 1. To perform MiL tests, the engine has been modeled in the GT-Power environment.

In the intake manifold, a  $O_2$  concentration sensor has been installed. Even if engine complexity grows, direct measurement allows for more precise monitoring of intake oxygen concentration. Furthermore, dynamic models can use the acquired data to make more precise output predictions.

The overall control structure is depicted in Fig. 2 and the three main blocks are briefly described in the next sections.

### A. Air path control

A NonLinear Quadratic Regulator (NLQR) controls the intake  $O_2$  concentration and IMAP by commanding the position of the EGR and VGT actuators. The designed control system incorporates two Nonlinear AutoRegressive with eXogenous input (NARX) Multiple Input Single Output (MISO) models. One network predicts the intake  $O_2$  concentration, while the other predicts the IMAP. Both have two hyperbolic tangent hidden neurons and a one-neuron linear output layer. The networks use five inputs: the actual values of the intake  $O_2$  concentration or IMAP, engine speed, engine BMEP, and the positions of the HP-EGR and VGT valves.

Recurrent Neural Networks (RNNs) allowed to use only a single model to identify the different I/O pairs nonlinear

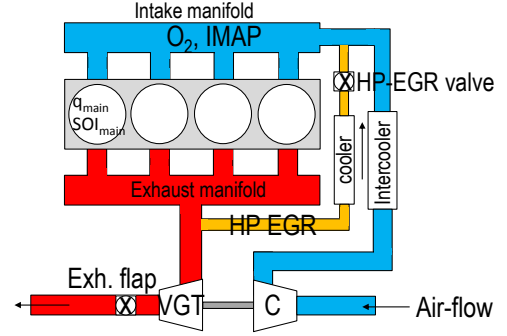


Fig. 1. Engine scheme.

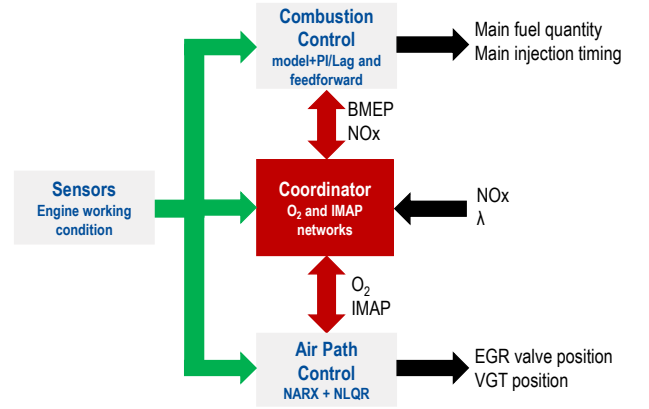


Fig. 2. Overall control structure.

correlations over the entire engine operating range. Furthermore, their low computational time suits for real-time ECU implementation. The details of the air path control system and embedded networks can be found in [13] and [14].

### B. Combustion control

A closed-loop combustion controller manages the diesel engine BMEP and NOx emissions. The two target variables are controlled by adjusting the injected main pulse fuel quantity  $q_{main}$  and timing (SOI). The closed-loop controller exploits the feedback from a predictive combustion model, used as a virtual sensor, that has been calibrated using actual test bench measurements. The model reconstructs a prediction of the in-cylinder pressure trace, which is then used to extract all the combustion metrics of interest. The model can reconstruct the pressure trace with or without physical sensor feedback. In the latter case, direct in-cylinder pressure measurement is not required.

The control system consists of two independent loops with PI and lag regulators, one to regulate engine load (BMEP), and the other to regulate NOx. Moreover, a feedforward term contribution enables the two command actions nominal steady-state values to be taken into account. The structure enables independent control of each of the four cylinders, resulting in the employment of eight regulators, two for each cylinder. [4] contains specifics about the feedback model, whereas [15] provides more detail about the control system.

### C. Coordinator

High level coordination of air path and fuel control systems becomes essential when the conflicting needs of emissions, fuel economy and driveability have to be met. The coordinator is the fulcrum of the combined engine air path and combustion management: it adapts control targets harmoniously in order to meet the different conflicting performance requirements. Model training and validation have been performed using the MATLAB Deep Learning Toolbox exploiting both experimental and simulated (by the GT-Power model) data. It is important to remark that the training is performed offline. The coordinator viability and functioning was assessed through software in the loop and MiL tests in co-simulation between Simulink and GT-Power.

In the structure shown in Fig. 2, a clear separation between the two control systems is visible. The coordinator sets the targets ( $O_2$  concentration and IMAP) for the air path controller, but acts in a different way on the combustion controller. The combustion control system receives as target the same NOx set point that the coordinator uses to generate the  $O_2$  reference, while the BMEP is imposed by the driver or by time varying profiles in simulation. It is important to remark that the red arrows in Fig. 2 are bidirectional. As a consequence, the coordinator not only sends the targets to the control systems, but at the same time receives feedback from them, producing targets in accordance with each other. The coordinator is intended to make the air path control system, the slowest, work as desired while the combustion controller compensates for the remaining faster target deviations. This allows the air path controller to provide the global conditions for the engine running and allowing the combustion control system to fulfill the requested torque. In addition, the combustion control compensates for fast variations and offsets in both load and NOx emitted pollutants.

In order to have complete control over the air path, a further feature characterizes its targets generation. The primary target is the intake  $O_2$  concentration that is strictly correlated to the NOx pollutant emissions. The second target, the IMAP, was chosen to be subjected to the  $\lambda$  (i.e., relative air-to-fuel ratio). In this manner, complete and separate management of the engine air path can be guaranteed and the control systems work coherently toward the same primary goal: NOx emission reduction. To this aim, two separate networks with runtime of the order of microseconds were used, one for the  $O_2$  and one for the IMAP. The first net inputs are the engine speed, engine BMEP,  $SOI_{main}$ , rail pressure, desired NOx and  $\lambda$  to produce an oxygen target. The second one uses injected fuel quantity,  $O_2$  and desired  $\lambda$  to generate an IMAP target. The network structure for the  $O_2$  reference generator is made of one input layer, eight hidden layers and one output layer (a typical shallow neural network), while for the IMAP it has one input layer, three hidden layers and one output layer. The structure of the networks has been chosen through multiple candidates of different complexity, i.e. number of neurons and inputs. By plotting the relative error over key-points of engine speed and engine load (i.e. over the engine map) the

networks performance can be evaluated over the same points used to characterize the engine. Therefore Figs. 3 and 4 show that the maximum relative errors for the  $O_2$  net are -2.5%, mainly above 2500 rpm, and +2%, at low load, while for the IMAP net they are -5.5%, at high load (above 12 bar) low speed (1250÷2000 rpm), and +2%.

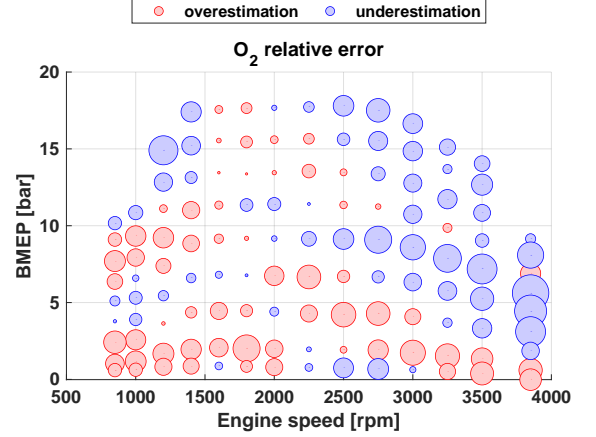


Fig. 3. Intake  $O_2$  concentration reference generator network relative error.

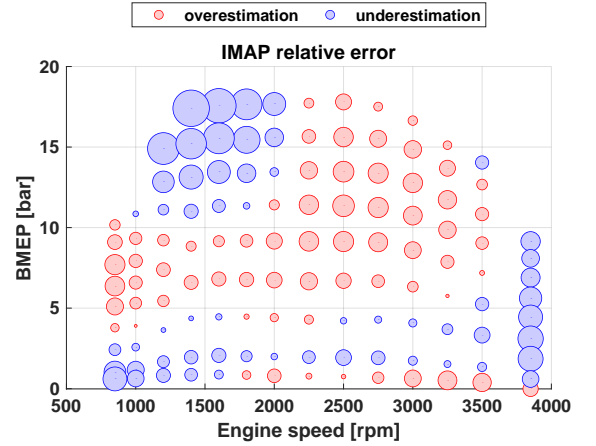


Fig. 4. IMAP reference generator network relative error.

Further details on the coordinator training and validation can be found in [16], while in the next section results of coordinated control systems are shown.

### III. RESULTS

Two distinct NOx calibration maps were used to impose two different NOx objectives in order to acquire the results here presented. As a consequence, two distinct references for  $O_2$  and IMAP are produced. It must be noted that the primary benefit of the suggested coordinated structure is the ability to define desired engine NOx and  $\lambda$  targets over the driving mission, which in turn leads to the definition of  $O_2$  and IMAP targets for the air path controller that are continuously adjusted in real time. By acting on the onset of the main pulse injection as well as the amount of fuel injected cycle by cycle, the combustion controller simultaneously corrects

for rapid fluctuations and offsets in both load and NOx released pollutants. The aim of the coordinator networks is to provide targets that take into account the physical dependence between the quantities which have been used as targets for the controllers. Furthermore, the engine-out NOx emissions, according to legislation, are considered as a cumulative quantity. Depending on the transient and the engine state, the instantaneous emission levels can change. The two targets simulate the different admissible emission levels depending on the engine working condition. Still, over a cycle, the integral of the emitted NOx have to be within the legislated limits. In the following figures the targets are referred to as “target 1” and “target 2” and the corresponding simulations are indicated through “sim 1” and “sim 2”. The engine load, BMEP, was imposed by a single time-varying profile, independent from NOx targets. Alike, the  $\lambda$  set point was the same for both simulations and provided by a map.

For the sake of brevity, only the simulations of a load hat ramp, Fig. 9, and a portion of the World Harmonized Transient Cycle (WHTC), Fig. 12, are discussed.

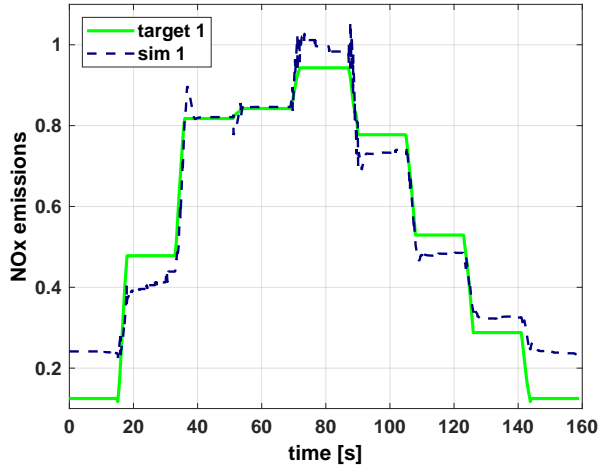


Fig. 5. Load ramp at 1500 rpm NOx simulation 1.

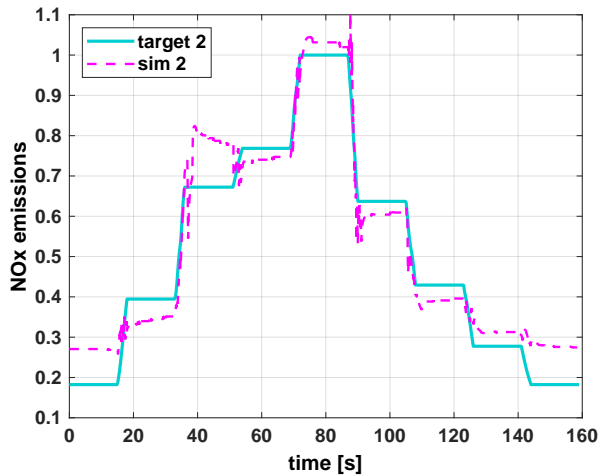


Fig. 6. Load ramp at 1500 rpm NOx simulation 2.

Analyzing the NOx data from the first simulation, Fig. 5 illustrates how the control system follows the target with the

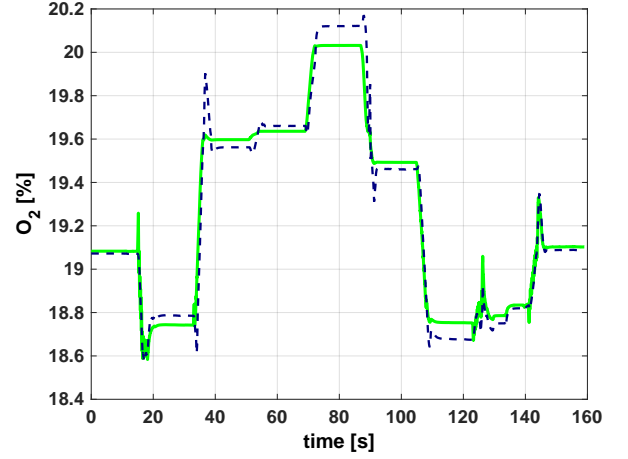


Fig. 7. Load ramp at 1500 rpm  $O_2$  simulation 1.

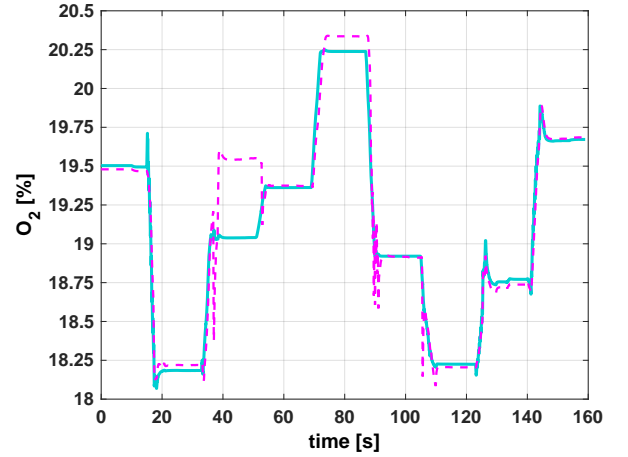


Fig. 8. Load ramp at 1500 rpm  $O_2$  simulation 2.

largest mismatches at the smallest load, in correspondence with the ramp tails. Looking at the outcome for the second target, Fig. 6, it is clear that the largest discrepancy from the target occurs between time  $t = 38$  s and time  $t = 46$  s. Finally, both NOx references are followed with a maximum deviation of 100 ppm, a value comparable to sensors precision.

By looking at the intake  $O_2$  concentration, Fig. 7, it is possible to see how the air path control system accurately follows the first target. The simulation of the second calibration, Fig. 8, presents a major mismatch from the target from time  $t = 38$  s to time  $t = 46$  s. This error is due to the air path control system that has reached its maximum allowed correction. Note that the portion of the ramp over which the oxygen deviates the most from the target, is the same where the highest NOx emissions error was recorded. This is a direct consequence of the strong relation between intake  $O_2$  concentration and NOx. A second noticeable behavior in this test is the jitter at time  $t = 85$  s during the first load drop, Fig. 8. This is due to the air path controller that stops correcting steady state maps, as their input produces large deviation from the target, and switches into pure optimization, see [13] for details.

The control system followed the load hat ramp with a

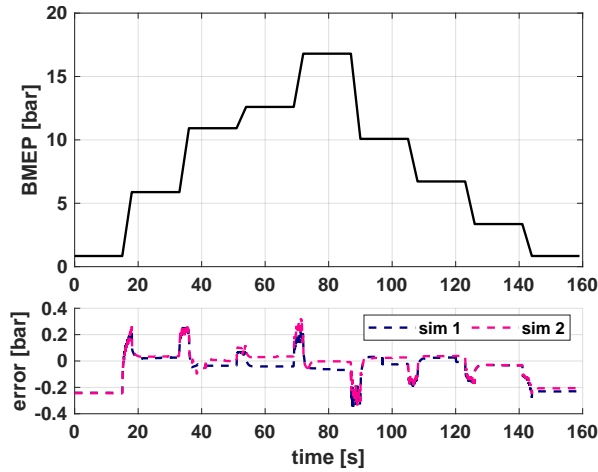


Fig. 9. Load ramp at 1500 rpm profile and errors.

maximum variation of  $\pm 0.3$  bar for both simulations, see the lower half of Fig. 9. The largest deviation occurs for a short period of time after the sharpest load variation at time  $t = 85$  s, corresponding to the previously stated jitter.

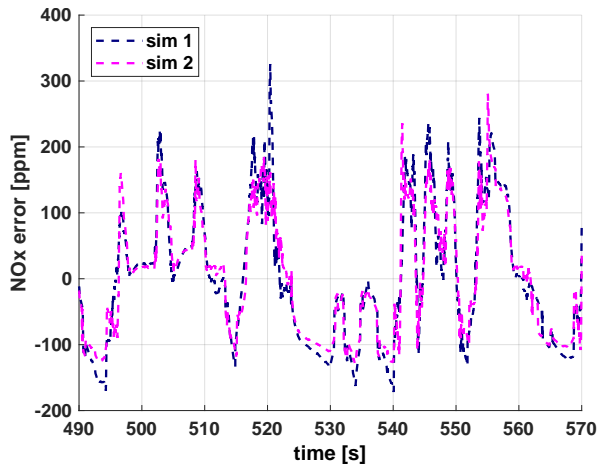


Fig. 10. WHTC NOx errors.

The second test that is being shown is a section of a WHTC that has been run twice with two different NOx objectives. The NOx errors throughout this cycle segment, shown in Fig. 10, are typically confined between  $-150$  and  $+250$  ppm for both calibrations. In line with the sharpest load fluctuations, more severe variances are only observed for brief periods of time. Overall, this slight deviation from the NOx target indicates that it is being closely observed. The total variance of the WHTC cumulative NOx emissions is  $\pm 5\%$ .

Both intake  $O_2$  concentration objectives resulting from the two NOx calibrations are accurately followed, as expected from the NOx error result, Fig. 11. Undershoots occur only during the most aggressive transients, in an attempt to follow the target, with the inaccuracy reaching 1.5% at time  $t = 540$  s. This discrepancy, however, is limited to the first samples of the transient maneuver.

Fig. 12 shows the BMEP target, upper portion, and the error for the two simulations, lower portion, for this section

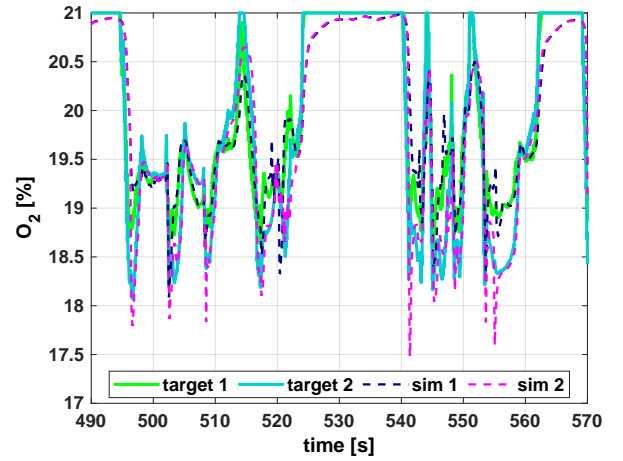


Fig. 11. WHTC  $O_2$ .

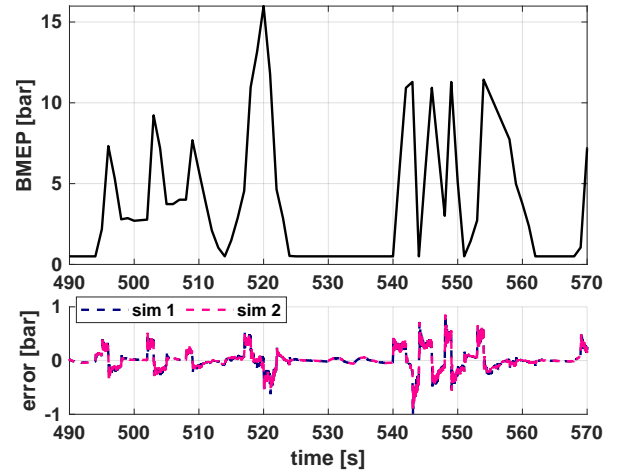


Fig. 12. WHTC BMEP profile and errors.

of the WHTC. The maximum error is of  $-0.98$  bar for sim 1 occurring at time  $t = 543$  s. Furthermore, it is visible that the error is higher when the BMEP variation is more severe, from time  $t = 540$  s to time  $t = 555$  s. An average error for the BMEP is around 0.45 bar.

By looking at Fig. 13, where the IMAP is shown, it is visible that the two targets imposed by the reference generator are very sharp as a reflection of the BMEP profile of this WHTC portion. The results of both simulations, blue and magenta, are very similar. Nonetheless, the second calibration shows a larger error due to the sharper target variations: in this case the error reaches 0.45 bar.

The  $\lambda$  value is shown in Fig. 14. The targets are equal since each simulation used the same steady state map where the  $\lambda$  reference value is recorded. When examining Fig. 14, it is instantly clear that there is a significant difference between the target and the two simulations. This occurs since the greatest  $\lambda$  value stored in the reference map is equal to 4. With the advent of the fuel control system, which lowers the amount of fuel that is injected,  $\lambda$  achieves values that are significantly greater than 4 in the low load regions. The creation of smoke is not the main issue in these circumstances, so the mismatch is not a problem. On the other hand, regardless of how quickly



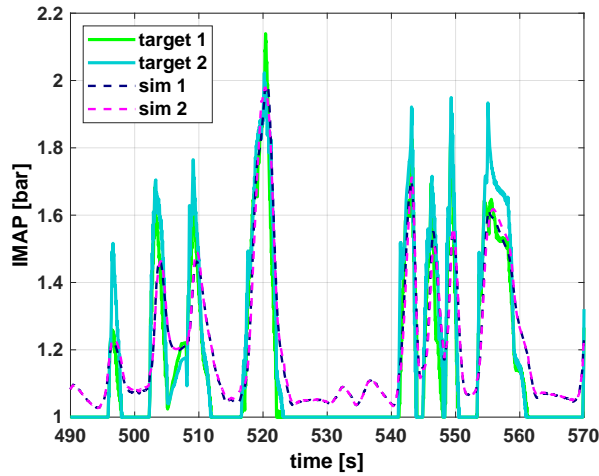


Fig. 13. WHTC IMAP.

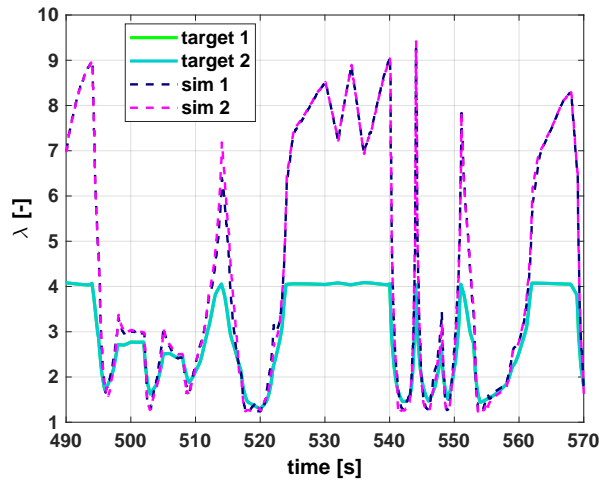


Fig. 14. WHTC  $\lambda$ .

the transient occurs, the  $\lambda$  objective is closely matched at a high load.

#### IV. CONCLUSIONS

In this work, an air path and combustion control systems coordinator, based on neural networks, has been tested to manage a heavy-duty diesel engine. The coordinator sets the targets for the two control systems, namely intake  $O_2$  concentration and IMAP for the air path and BMEP and NOx for the combustion. The air path  $O_2$  target is generated considering a desired NOx set point and the engine and combustion control states through engine speed and load, rail pressure and SOI. Instead, the IMAP target is generated given desired  $\lambda$ , intake  $O_2$  and injected fuel. The same load and NOx targets used for the air path targets generation are also sent to the combustion control systems.

Simulated results were encouraging, with good accuracy in tracking the NOx targets. The structure effectively enabled the tracking of different NOx targets, with an average inaccuracy of 0.3 bar for the BMEP and 100÷150 ppm for the NOx. The IMAP deviations from targets were affected by the  $\lambda$  regulation. Yet, during high loads, when it mattered the most,

the control was extremely accurate, never falling below  $\lambda = 1.2$ . In conclusion, the simulations demonstrated the viability and excellent performance of the approach.

Future research will evaluate the approach viability by applying the logic to a fast prototyping device and using a NOx target that changes dynamically across the transient.

#### ACKNOWLEDGMENT

Profs. Stefano d'Ambrosio and Roberto Finesso (Energy Department, Politecnico di Torino) provided valuable support to the authors in developing and revising this work.

#### REFERENCES

- [1] M. Baratta, R. Finesso, D. Misul and E. Spessa, "Comparison between internal and external egr performance on a heavy duty diesel engine by means of a refined 1D fluid-dynamic engine model," *SAE International Journal of Engines* Vol. 8, No. 5 (November 2015), pp. 1977-1992.
- [2] A. Ferrari, Z. Jin, O. Vento and T. Zhang, "An injected quantity estimation technique based on time-frequency analysis," *Control Engineering Practice*, vol. 116, 2021.
- [3] S. D'Ambrosio, F. Gaia, D. Iemmolo, A. Mancarella, N. Salamone, R. Vitolo and G. Hardy, "Performance and emission comparison between a conventional euro VI diesel engine and an optimized PCCI version and effect of EGR cooler fouling on PCCI combustion," in *WCX World Congress Experience*. SAE International, apr 2018.
- [4] R. Finesso, O. Marelli, E. Spessa, Y. Yang and G. Hardy, "Model-Based Control of BMEP and NOx Emissions in a Euro VI 3.0L Diesel Engine," In *SAE Int. Journal of Engines*, vol. 10, 2017.
- [5] A. Ferrari, C. Novara, E. Paolucci, O. Vento, M. Violante and T. Zhang, "Design and rapid prototyping of a closed-loop control strategy of the injected mass for the reduction of CO<sub>2</sub>, combustion noise and pollutant emissions in diesel engines," In *Applied Energy*, vol. 232 2018, pp. 358-367.
- [6] G. Landsmann, M. Beasley, R. Cornwell, P. Fussey, R. King, A. Noble, T. Salamon and A. Truscott, "Reducing Diesel Emissions Dispersion by Coordinated Combustion Feedback Control," In *SAE 2006 World Congress & Exhibition*.
- [7] B. Shin, Y. Chi, M. Kim, P. Dickinson, et al., "Model Predictive Control of an Air Path System for Multi-Mode Operation in a Diesel Engine," *SAE Technical Paper* 2020-01-0269, 2020.
- [8] L. Yin, G. Turesson, P. Tunestål and R. Johansson, "Model Predictive Control of an Advanced Multiple Cylinder Engine With Partially Premixed Combustion Concept," In *IEEE/ASME Trans. on Mechatronics*, vol. 25, no. 2, pp. 804-814, April 2020.
- [9] S. A. Malan and L. Ventura, "Air-Path Control for a Prototype PCCI Diesel Engine," In *Proc. of 2018 26th Mediterranean Conference on Control and Automation*, pp. 843-848, 2018.
- [10] L. Ventura, R. Finesso, S. A. Malan, S. d'Ambrosio and A. Manelli, "Model-based design of closed loop controllers of the air-path in a heavy duty diesel engine," In *74th Congresso Nazionale ATI*. AIP Conference Proceedings, sep 2019.
- [11] T. Albin, D. Ritter, R. Zweigel and D. Abel, "Hybrid multi-objective MPC for fuel-efficient PCCI engine control," In *Proc. of 2015 European Control Conference*.
- [12] I. Abidi, J. Bosche, A. E. Hajjaji and A. Aguilera-Gonzalez, "Fuzzy robust tracking control with pole placement for a Turbocharged diesel engine," In *Proc. of 21st Mediterranean Conference on Control and Automation*, pp. 1417-1422, 2013.
- [13] L. Ventura and S. A. Malan, "NLQR Control of High Pressure EGR in Diesel Engine," In *Proc. of ICCAS 2020 20th International Conference on Control, Automation and Systems*.
- [14] L. Ventura and S. A. Malan, "Intake O<sub>2</sub> Concentration Estimation in a Turbocharged Diesel Engine through NOE," In *SAE Int. J. Adv. & Curr. Prac. in Mobility* 3(2):864-871, 2021.
- [15] S. A. Malan, L. Ventura and A. Manelli, "Cycle to cycle closed-loop combustion control through virtual sensor in a diesel engine," In *Proc. of 2021 29th Mediterranean Conf. on Control and Automation*.
- [16] L. Ventura, and S. A. Malan, "Air path and combustion controllers coordination for diesel engine," In *Proc. of ICCAS 2022 22nd International Conference on Control, Automation and Systems*.